Annales Geophysicae, 23, 1103–1121, 2005
SRef-ID: 1432-0576/ag/2005-23-1103

Annales Geophysicae

Planetary wave coupling in the middle atmosphere (20–90 km): A CUJO study involving TOMS, MetO and MF radar data

T. Chshyolkova[1], **A. H. Manson**[1], **C. E. Meek**[1], **S. K. Avery**[2], **D. Thorsen**[3], **J. W. MacDougall**[4], **W. Hocking**[4], **Y. Murayama**[5], **and K. Igarashi**[5]

[1]Inst. of Space and Atmospheric Studies, Univ. of Saskatchewan, 116 Science Place, Saskatoon, SK, S7N 5E2, Canada
[2]CIRES, University of Colorado, Boulder, USA
[3]Department of Electrical and Computer Engineering, University of Alaska, Fairbanks, USA
[4]Department of Physics and Astronomy, University of Western Ontario, London, Canada
[5]National Institute of Information and Communications Technology, Tokyo, Japan

Received: 3 June 2004 – Revised: 9 February 2005 – Accepted: 28 February 2005 – Published: 3 June 2005

Abstract. The atmospheric coupling due to Planetary Waves (PW) in the middle atmosphere (20–90 km) has been studied using TOMS, MetO and MFR data. The wavelet and wave number analyses have been applied to all parameters at five CUJO (Canada US Japan Opportunity) locations. The CUJO network covers latitudes of 31–52° N and longitudes from 81° W to 142° E, and allows for the assessment of longitudinal variability. The results of temporal and spectral comparisons show that the total ozone (TOMS) and MetO temperatures at low stratospheric heights (typically 100 mbar) have high values of correlation as well as similar spectral content. The eastward motions dominate at low stratospheric heights (100 mbar), while westward motions became comparable or even stronger in the upper stratosphere (0.46 mbar). During the summer months a reduction of PW activity has been observed in the stratosphere, especially at its upper heights, and in the upper middle atmosphere. The MetO (0.32 mbar, 55 km) and MFR winds (circa 60 km) are in good general agreement, especially for the zonal component. Several examples of planetary wave activity at different atmospheric levels throughout the middle atmosphere have been presented. These examples include an eastward propagating 15-day disturbance with wave number 6, that has been observed only at low stratospheric heights; long-period (20–30 days) oscillations with wave number ∼1 that have been detected in a wide height range (20–90 km); and an oscillation with period near 16 days that was found only at mesospheric heights.

Keywords. meteorology and atmospheric dynamics (Middle atmospheric dynamics; Waves and tides)

Correspondence to: T. Chshyolkova
(t.sch@usask.ca)

1 Introduction

The Mesosphere/Lower Thermosphere (MLT, 50–100 km) region is known for its great variability. At any moment the mesospheric observations contain a mixture of gravity waves, tides and planetary waves; and the amplitudes of these waves vary significantly with time. This variability can be produced in situ, for example due to non-linear wave interactions, and/or be brought in from outside the region. In particular, the influence of the lower atmospheric regions is substantial. Due to a lack of observations, which would have to cover a large altitude range at many geographical locations, as well as due to the complexity of the atmospheric processes themselves, different atmospheric regions are quite often considered separately. Although there are still not enough observational data at MLT heights, the development and improvement of numerical models and assimilated techniques over the last 10–15 years have helped to provide evidence for coupling between different atmospheric regions. Several coupling processes, such as vertical Planetary Wave (PW) propagation, ducting of PW from the other hemisphere, nonlinear PW-tide interactions, disturbances in MLT tides associated with fluctuations in the total ozone forcing, and Gravity Wave (GW) propagation, have been named and illustrated in the literature (e.g. Pancheva et al., 2003; Manson et al., 2005).

Recently several papers, which involve both the lower and middle atmosphere, have been published. Smith (1996) and (2003) have demonstrated the importance of coupling by GW using the High Resolution Doppler Imager (HRDI) measurements and model calculations. Significant portions of the GW spectrum generated in the troposphere can propagate vertically. On their way up they are filtered due to interaction with stratospheric winds associated with PW. Those GW that reach mesospheric heights generally dissipate and deposit momentum, and as a result can generate planetary-scale disturbances in situ.

Pancheva et al. (2003) investigated variations (3–100 days) of the semidiurnal (12 h) tide observed in the MLT region by the meteor radar located in Sheffield (53° N). Among other results, they have shown that during winter the amplitude modulations of the semidiurnal tides have periods ∼10, ∼16 and ∼25–28 days, and that similar temporal variations have been simultaneously present in the total ozone. The phase relationships between variations in total ozone (in the lower stratosphere) and those in 12 h tide (in the MLT) suggested that in most of the cases the amplitude modulations of the semidiurnal tides observed in the MLT region were mainly produced by non-local coupling between the semidiurnal tide and PW in the stratosphere. Also, in the case of relatively long time lags, similar variations in the considered regions can be attributed to local nonlinear interactions between the tides and PW in the MLT.

Manson et al. (2005) continued investigation of the atmospheric variability with PW periods (2–30 days) in total ozone, background MLT winds, and semidiurnal (12 h), as well as, diurnal (24 h) tides using satellite (TOMS) and Medium Frequency (MF) radar data from the CUJO network (5 radars, 31–52° N, Pacific-North America). The results have indicated that the character of variability at PW periods for the tidal amplitudes differs from that of the mean winds, which could be explained by different sources for their variability. However, there were some events that demonstrated oscillations at planetary wave periods in both the tides (12-, 24-h) and winds of the MLT, and in the total ozone data, at the middle latitude stations. Mechanisms discussed included non-linear coupling, ozone and GW forcing. The spectral character of the coupling between the 24 h tide of the MLT and the total ozone suggests that the PW-tides local and/or non-local interactions are often sources of tidal variability at the MLT heights, but that the ozone variability should also be considered as a forcing mechanism. It was noted that even though the ozone is not the dominant forcing mechanism for the 24 h tide, it still plays a significant role (Hagan, 1996).

Planetary waves (PW) are often generated in the lower atmosphere and may propagate upward carrying energy and momentum, thus providing dynamical coupling between the lower and middle atmosphere. Lawrence and Randel (1996) examined the variability of daily temperatures, geopotential heights, and "balance-wind" estimates that have been retrieved from the radiance data measured by the pressure modulator radiometer (aboard Nimbus 6). They found strong evidence of coupling between the stratosphere and mesosphere (30–85 km) for daily variations of the zonal-mean flow and for "wave-like events". However, the authors have noted that not all wave-like disturbances seen in the mesosphere are due to propagation from below. The idea of complex relationships between planetary wave activity in different atmospheric regions has also been supported by Lawrence and Jarvis (2003), who studied PW with near 16-, 10- and 5-day periods using ECMWF (The European Centre for Medium-Range Weather Forecasts) assimilative operational analysis and a High Frequency (HF) radar located at Halley (76° S, 27° W), Antarctica. It was demonstrated that simple vertical propagation of PW could not explain the observed picture of planetary wave activity at different atmospheric levels. The in-situ generation of planetary waves and PW-tide or PW-GW interactions have been suggested as possible additional mechanisms.

Following Manson et al. (2005) we continue the investigation of the seasonal variation of coupling due to PW in the middle atmosphere (20–95 km). As mentioned above, the previous study involved two different parameters: the total ozone and MFR winds (85 km). Although the total ozone is quite often used as an indicator of PW activity at lower stratospheric or tropopause heights, it is selective, e.g. the maximum signal in total ozone is thought to be produced by evanescent waves near the tropopause (Schoeberl and Krueger, 1983), while the influence of waves with shorter vertical wavelengths will not be as evident. The large altitudinal gap between the ozone and radar heights is another concern. To eliminate these uncertainties the MetO (also well known as UKMO: UK Meteorological Office) assimilated fields are used in this study. The description of the data sets is given in Sect. 2. The comparisons of time sequences and spectral analyses appropriate to these data sets and hence to different altitudes in the middle atmosphere are presented in Sects. 3 and 4, respectively. Some wave number studies are provided in Sect. 5, and there is a summary in Sect. 6.

2 Data sets

This study has involved several sets of data over three years 2000–2002. Medium Frequency (MF) radars at London (43° N, 81° W), Platteville (40° N, 105° W), Saskatoon (52° N, 107° W), Wakkanai (45° N, 142° E) and Yamagawa (31° N, 131° E) provide wind data from near 60 to 100 km. These radars form the CUJO network (Canada U.S. Japan Opportunity). The MF radars, which employ spaced antenna arrays, measure the atmospheric winds using partial reflections or scatter from weakly ionized irregularities in the ionospheric D region and lower E-region. All five MF radars are of similar configuration. As an example, consider the MF radar located in Saskatoon. The system utilizes pulsed radiowave transmissions of 2.2 MHz, with a pulse width of 20 μs, repetition rate of 60 Hz (17 ms), and peak power of approximately 25 kW. The transmitting antenna array consists of 16 half-wave dipole elements. Three receiving antenna systems are arranged in the form of an equilateral triangle of side 2λ with another antenna in the middle. This MF radar, as well as those located at London and Platteville, samples the partial reflections at time intervals of 5 min and at 3 km height intervals on a continuous basis. The spaced antenna "full correlation analysis" method (Meek, 1980) has been used to calculate wind velocities (at London slightly different software was used). Other MF radars located in Japan operate at 2.0 MHz and have 2 min time and 2 km height sampling intervals. Although a more classical method of analysis described by Briggs (1984) has been used in this case, the results of comparisons (Thayaparan et al., 1995) suggest no significant difference between the two methods. The detailed description of these radars can be found elsewhere (Manson et al., 1973; Thayaparan et al., 1995; Igarashi et al., 1999). The daily mean data from each sampled height have been employed for the wind analyses in this paper. The 5- or 2-min data were first used to obtain the hourly mean winds, which, in turn, have been averaged over the day. These values are considered to be valid if there are at least 2 values within an hour and at least 6-hourly mean values per day. Usually the coverage is poorest at low heights (due to the lack of radar scatter during the night below 70 km), but becomes better near and above 80 km, where the number of hourly mean values approaches 24 (Luo et al., 2002a).

The second data set is daily "total ozone column" data. The Total Ozone Mapping Spectrometer (TOMS) on board the Earth Probe (EP) satellite measures the total number of ozone molecules between the surface of Earth and the top of the atmosphere. The amount of ozone in this column is numerically expressed in Dobson Units. The daily product is available with a fixed global grid, which is 1 degree in latitude by 1.25 deg in longitude. The total ozone (hereafter this phrase or "ozone" is used) daily samples for any particular location are measured near local noon. The official TOMS website, http://jwocky.gsfc.nasa.gov/, offers more detailed information about their data.

Other sets of data that have been used are stratospheric fields of daily temperature and wind components (at 12:00 UTC) provided by the UK Meteorological Office (MetO) from the British Atmospheric Data Center (BADC) website at http://badc.nerc.ac.uk. These data have global coverage with 2.5° latitudinal and 3.75° longitudinal steps and are available for 22 pressure levels from 1000 mbar to 0.316 mbar (∼0–55 km). Basically, observational data are continually incorporated in a global circulation model (GCM) using the assimilation system (Lorenc et al., 1991; Swinbank and O'Neill 1994a; Lorenc et al., 2000), and updated atmospheric samples of temperatures, winds and pressure are made available with daily temporal resolution. The GCM used by UK Met. Office is based on a set of primitive equations and incorporates several physical parameterizations (see Swinbank et al., 1998 or http://metoffice.com/ for more details) including GW parameterization (Warner and McIntyre, 1999) since year 2000.

The MetO analyses represent the major features of atmospheric circulation quite well. For example, the global fields include quasi-biennial and semi-annual oscillations at low latitudes (Swinbank and O'Neill, 1994b), and the quasi 2-day wave and an inertial circulation (Orsolini et al., 1997). The comparisons of MetO and SABER (the Sounding of the Atmosphere using Broadband Emission Radiometry) temperatures show very good agreement (Remsberg et al., 2003).

Recently the results of a detailed intercomparison of climatological datasets for the middle atmosphere that are currently used (MetO, UKTOVS, CPC, NCEP, ERA-15, ERA-40, FUB, CIRA86, HALOE, MLS, URAP) have been published (Randel et al., 2004). It was shown that in general there are overall good agreements between datasets. However each dataset has weaknesses, or "can exhibit 'outlier' behavior for certain statistics". In particular for the MetO dataset, cold temperature biases (∼5 K) near the stratopause (the upper boundary of the dataset) and warm tropical tropopause temperatures (1–2 K) have been named. Note, however, that the data used for these comparisons are from earlier years (1992–1997), before the later improvements in the model and the assimilation technique.

3 Time sequences of MetO, MFR and TOMS data

Different mechanisms account for variations in ozone concentration at different altitudes. At low stratospheric heights dynamic processes control ozone concentration, while photodissociation becomes more significant in the upper stratosphere (Salby, 1996). However, taking into account the fact that ozone is not evenly distributed with height but is concentrated in the stratosphere, total ozone data have been frequently used to characterize planetary wave activity at stratospheric heights. The availability of MetO parameters at 22 pressure levels from the surface to ∼55 km makes it possible to test whether the total ozone has a simple correlation with temperature and/or horizontal wind components at any particular level in order that we can use one of the MetO parameters to represent the total ozone.

Time sequences of MetO temperatures for several heights/pressure levels at the latitude and longitude of Saskatoon during 2001 have been plotted in Fig. 1. For convenient comparisons the total ozone variations are shown by dashed lines along with temperature sequences (solid lines). The horizontal time-axis lines represent the means for both temperature and the total ozone data, but different scales have been used to plot temperature and ozone data to make their variations comparable. As seen from the figure, the variations of the total ozone and temperature could be out of phase (at ∼464 mbar), in phase (∼100, 215 mbar), or exhibit complex relations (above ∼10 mbar). A similar picture is observed for all three (2000–2002) years and all locations for the CUJO network. To generalize, the cross-correlation coefficients have been calculated for all MetO parameters used in this paper and the total ozone. For the calculations a window of 30 days and a 10-day sequential step have been employed. Each 30-day time interval has been linearly detrended.

The resultant contour plots of cross-correlation coefficients between temperature and the total ozone versus height and time (2001 year) for three (Saskatoon, Platteville, and Yamagawa) CUJO locations are shown in Fig. 2. Positive and negative values are shown by solid and dashed curves, respectively, with 0.2 steps between contours. All stations exhibit this regular pattern in all years: negative correlations at low heights change to positive correlations in the altitude range from ∼10 to 25–30 km, while in the upper stratosphere the cross-correlation coefficients are not high and change sign with time. This result is not new and agrees

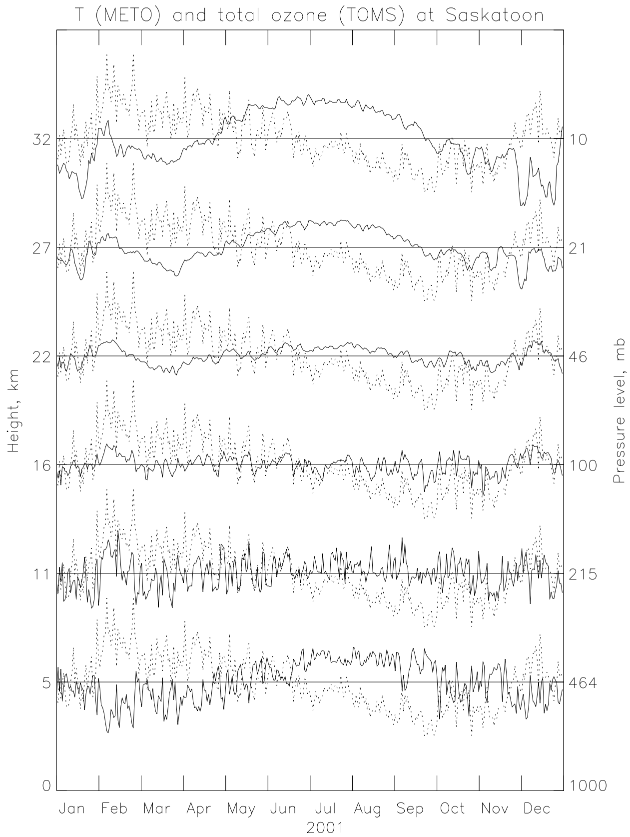

Fig. 1. The variations of total ozone (dashed line) and MetO temperatures (solid lines) at several heights/pressure levels for Saskatoon, 2001. For convenient comparison the variations of total ozone are shown for each height/pressure level. Different scales have been used to plot ozone (200 DU per division) and temperature (40 K per division) variations to make them comparable.

well with strong correlations between atmospheric temperatures and total ozone found for variations with different time-scales in other studies (Hood et al., 1997; Ziemke et al., 1997; and references therein). (Such correlation analysis using the MetO assimilation products is new however). Horizontal winds have smaller cross-correlation coefficients and irregular structures with time and height (not shown), suggesting a more complex relation with total ozone. Therefore it is reasonable to assume that the total ozone and the temperature at low stratospheric heights have similar temporal variations. Spectral characteristics will be investigated later.

We now compare MetO and MF radar winds, as this will speak to the value of the data assimilation product at the top of the dataset. Such comparison is new. Zonal components (east-west) of the MetO (low panel) and MF radar (middle panel) horizontal winds are shown in Fig. 3. There is very good general agreement for the transition heights between two data sets: the winds are westward in summer and eastward in winter with clear equinox transitions. The strong dynamical events, such as those associated with stratospheric warmings, are also evident in both data sets. For example, during the "stratwarm" that occurred from the end of January to the beginning of February 2000 ("stratalert" information at ftp://strat50.met.fu-berlin.de/pub/stratalert/1999_2000) both MetO and MF radar data sets show a reversal in the zonal (Fig. 3) and meridional winds (not shown). On the other hand, the speeds near 55 km from MetO and MFR did not initially agree well. Several previous comparisons of the MF radar winds with those from rockets (Meek and Manson, 1985) at similar heights, and Fabry-Perot interferometer (Manson et al, 1996), meteor radars (Cervera and Reid, 1995; Hocking and Thayaparan, 1997), and satellite data (Meek et al., 1997) at mesopause heights (80–100 km) have shown that while there is good agreement in the direction of the winds, the speeds measured by MF radars are systematically low by factors of typically 1.5. To account for this discrepancy, the MF radar winds for Fig. 3 have been multiplied by a 1.5 factor before plotting. With the adjustment the speeds recorded by the two systems are quite similar. Another comparison of MetO assimilated winds with observations has been presented by Burrage et al. (1997). They have reported that despite some differences there is also very close agreement between monthly zonally averaged zonal winds in the stratosphere (15–40 km) measured by HRDI and predicted by the MetO (which is mainly based upon radiosonde data). Later, HRDI and MetO (up to 1 mbar) winds ("balanced" values were calculated at the top of the MetO dataset) were combined to produce a data set that describes the monthly zonal mean zonal winds from the surface to the upper mesosphere (Swinbank and Ortland, 2003).

In the upper panel the contours of the cross-correlation coefficients between the winds at the highest MetO pressure level (0.32 mbar) and MF radar winds at 58 km are shown. The correlation coefficients have been calculated in the same way as described above. Maximum values tend to occur near zero lags in all seasons. Without detrending the cross-correlation coefficient would be highest during equinox transitions. The slight shift of the maximum cross-correlation coefficients from lag=0 toward lag=1 day could be due to the 7-h shift between MetO (12:00 UT) winds and Saskatoon daily winds defined as 24 h of local time. The relatively low correlation coefficients, and their time shift, could be also explained by the potential poorer reliability of the daily data parameter at the highest MetO and lowest MF radar levels.

4 Spectral comparison of MetO, MFR and TOMS data

In this section the spectral characteristics of the data have been studied using the wavelet technique. One of the popular wavelets, called the Morlet wavelet (Kumar and Foufoula-Georgiou, 1997), has been used. The Morlet wavelet is basically a sinusoid modulated by a Gaussian:

$$\psi(t) = \pi^{-\frac{1}{4}}(e^{-i\omega_0\eta}e^{-\frac{\eta^2}{2}}),$$

$$\eta = {(t-\tau)}/{s},$$

where τ is the time location of the localized transform and s is the scale factor that dilates or contracts the wavelet scale.

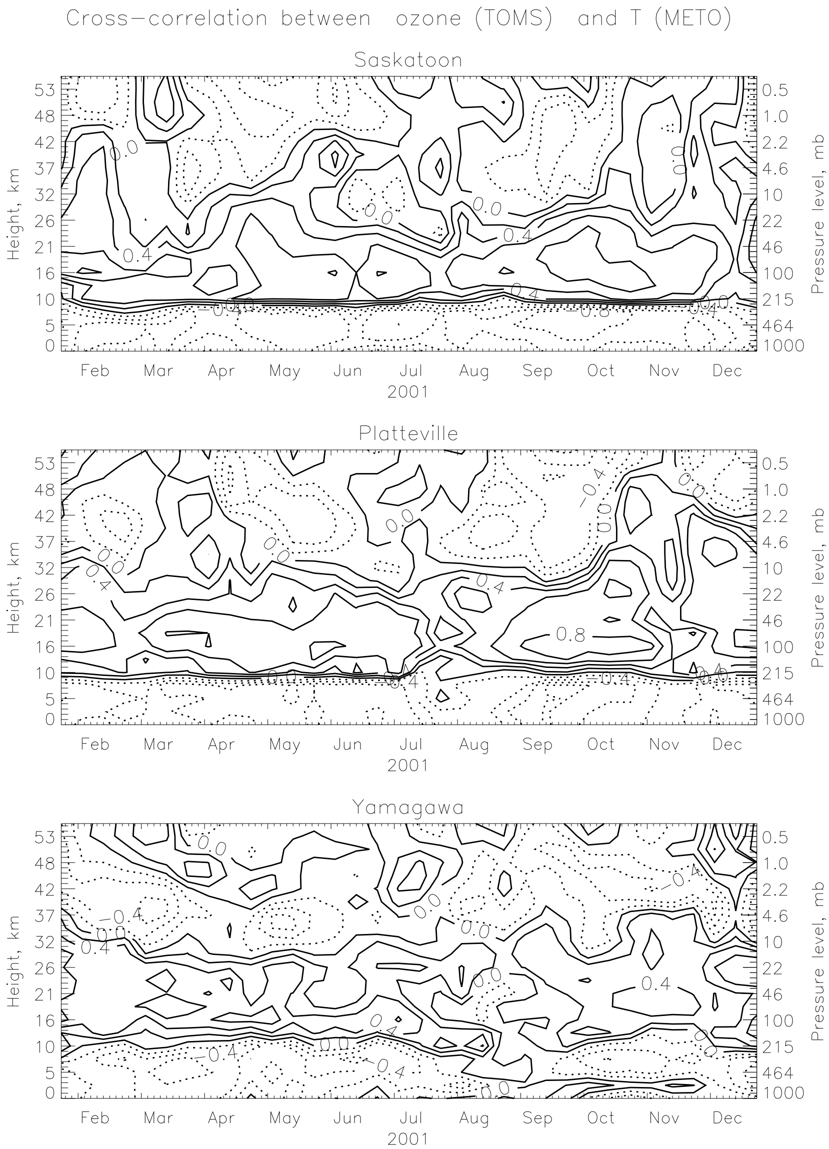

Fig. 2. The linear cross-correlation coefficients of the total ozone (TOMS) and temperature (MetO) versus time and height for three stations: Saskatoon (the top panel), Platteville (the middle panel), and Yamagawa (the bottom panel). The step between contours is 0.2.

The nondimensional frequency, so-called "wave number", (ω_0) was chosen equal to 6. By changing the scale, s, and moving along the time, τ, the amplitudes of oscillations at selected periods (2–30 days) are calculated. The calculations have been adopted from Torrence and Compo (1998), in which the scale parameters have been chosen as

$$s_j = s_0 2^{j\delta j}, \quad j = 0, 1, ..., J$$
$$J = \delta j^{-1} \log_2(\frac{N\delta t}{s_0})$$

s_0 is the smallest scale equal to 2δt (2 days in our case), N is the total number of points, and δj is equal to 0.125 (8 subscales). In general the wavelet scale is not equal to the period (Fourier transform) of the oscillations. For the Morlet wavelet with ω_0=6 the ratio between the Fourier period and the wavelet scale is 1.03. Comparisons with Lomb-Scargle spectra, for which significance levels are readily available (e.g. Luo et al., 2002b), indicate that spectral peaks of greater than 4 m/s amplitude are significant at >90% levels. We have repeated and confirmed these calculations, and applied them to the normalized amplitudes of the figures (see below).

All plots presented in this section are the wavelet-normalized amplitudes (in general well-formed peaks of greater than 0.4 are significant at >90%) versus time and period. The results are shown for all five CUJO locations with the Saskatoon (52° N) at the top, Yamagawa (31° N) at the bottom, and Platteville, London and Wakkanai (40–45° N) in the middle. Note that the top and the bottom pairs of locations have almost common longitudes and provide effectively only latitudinal change, while the three middle locations have almost common latitudes and a wide range (1000–7000 km)

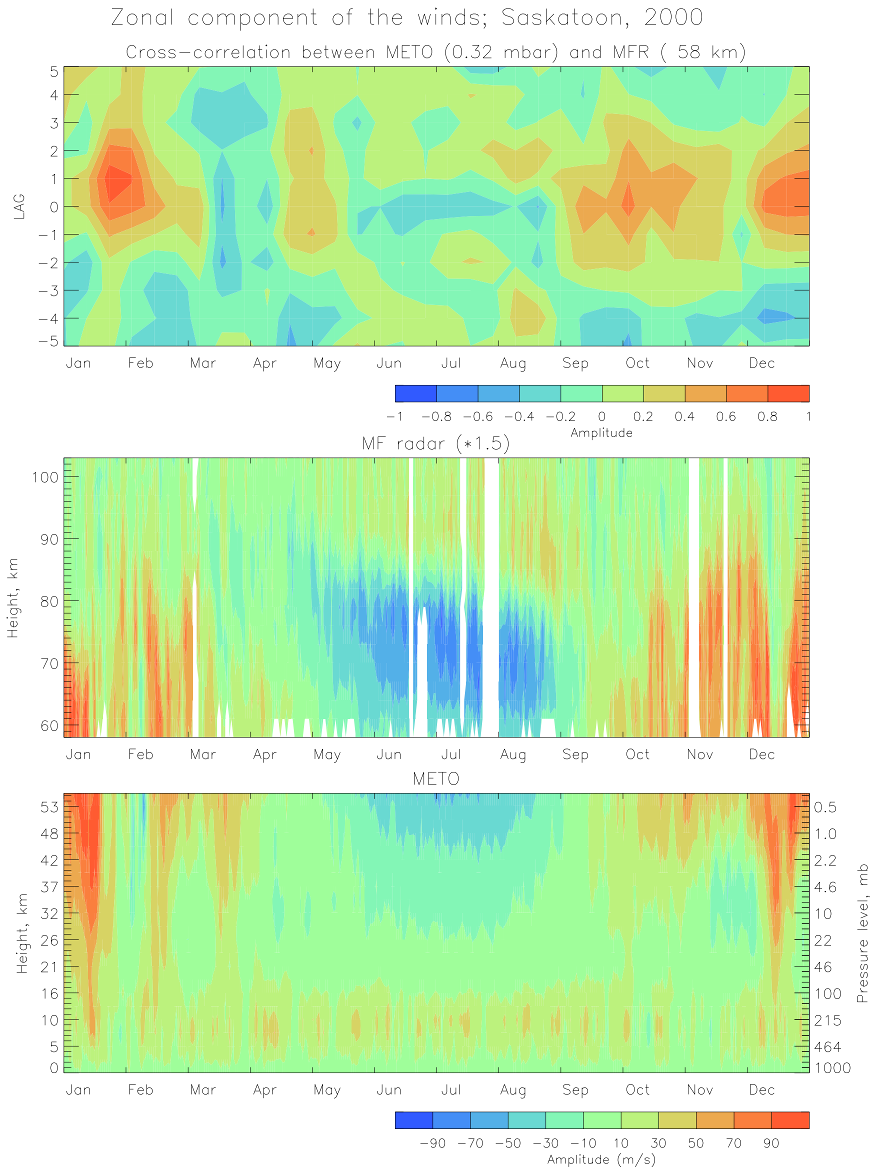

Fig. 3. The contour plots of zonal winds from MetO (the bottom panel) and MF radar (the middle panel) for Saskatoon during 2000. The cross-correlations calculated between the MetO winds at 0.32 mbar and MF radar winds measured at 58 km are shown on the upper panel.

of longitudes. The first two columns are wavelets of two different parameters, and the third column is their cross-product. Due to the best data coverage, year 2001 has been chosen for demonstration. Assessment of other years, from our extensive data set at Saskatoon, indicates that this year is quite typical. However, the comparison of MetO (0.46 mbar) and MFR (82 km) is also presented for year 2002 to show that the spectral contents of the data exhibit a modest interannual variability and the results of comparisons are consistent from year to year. The model and assimilation method was also the same for 2001 and 2002.

The oscillations of the zonal mean (average around a latitude circle) fields (T and U, in particular) can have large amplitudes in the stratosphere at mid- and high latitudes. To account for the effects of these oscillations the calculations have been carried out for MetO data with and without the subtraction of zonal mean values. The resulting wavelets showed the dominant peaks even clearer, while the cross-products had no significant differences. In general the zonal mean fields fluctuate with large periods, >20–30 days, that are the upper limit of spectra used in this paper. Considering the impossibility of a separation of the zonal mean and residual mesospheric winds, the zonal mean values were not removed from the daily local MetO data.

We first compare wavelets of the total ozone and MetO temperature at 100 mbar (Fig. 4). According to the result obtained in Sect. 3, the MetO temperatures in the height region from 10 to 26 km (∼215 to ∼46 mbar) have the highest positive correlation with the total ozone. As can be seen from Fig. 4, both parameters have similar dominant

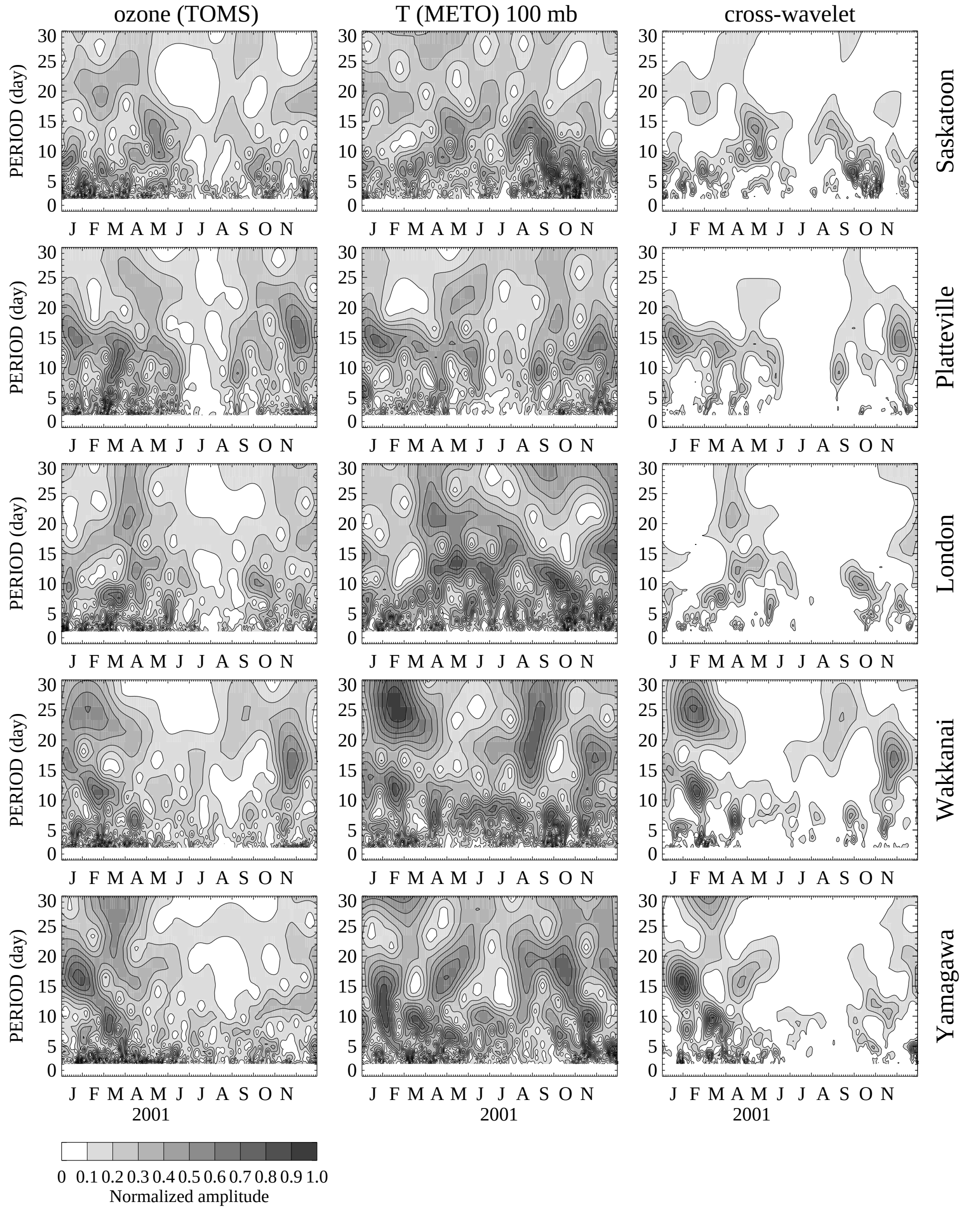

Fig. 4. The self-normalized wavelet amplitudes versus time (2001 year) and period (2–30 days) calculated for the total ozone (the left column) and MetO temperature at 100 mbar (the center column), and their cross-products (the right column) are presented for all five CUJO locations. From the top to the bottom these are for Saskatoon, Platteville, London, Wakkanai, and Yamagawa.

spectral components, and in most cases amplitude maxima in the cross-products are the results of contributions from spectral maxima in both the temperature and the total ozone. The main difference between these parameters, true for all CUJO locations, is the relatively low spectral amplitudes (hereafter, activity) in the total ozone during late summer. The total ozone not only reaches a minimum during July/August, but it also has smaller variability at that time than during the rest of the year (also see Fig. 1). Figure 4 is also interesting in the context of the recent paper by Manson et al. (2005) (see Introduction) due to these spectral differences; however very small differences in their results are expected, as the summer PW activity is also small in the MFR wind wavelets. Comparing different locations, the wavelets of the temperature at 100 mbar pressure level and of the total ozone, as well as their cross-products, show few if any similarities between stations. This suggests that the waves connected with these periods are either of small scale, or are localized in latitude (e.g. Luo et al., 2002b). However, cross-wavelets for Platteville and Wakkanai have features near 10–15 day in both winters.

Now consider Fig. 5, where the spectral variability in temperature is shown for two heights: 100 and 0.46 mbar. The character of the variability at 0.46 mbar pressure level has changed in comparison with the lower level, as there is now a strong reduction in spectral intensity in the summer months.

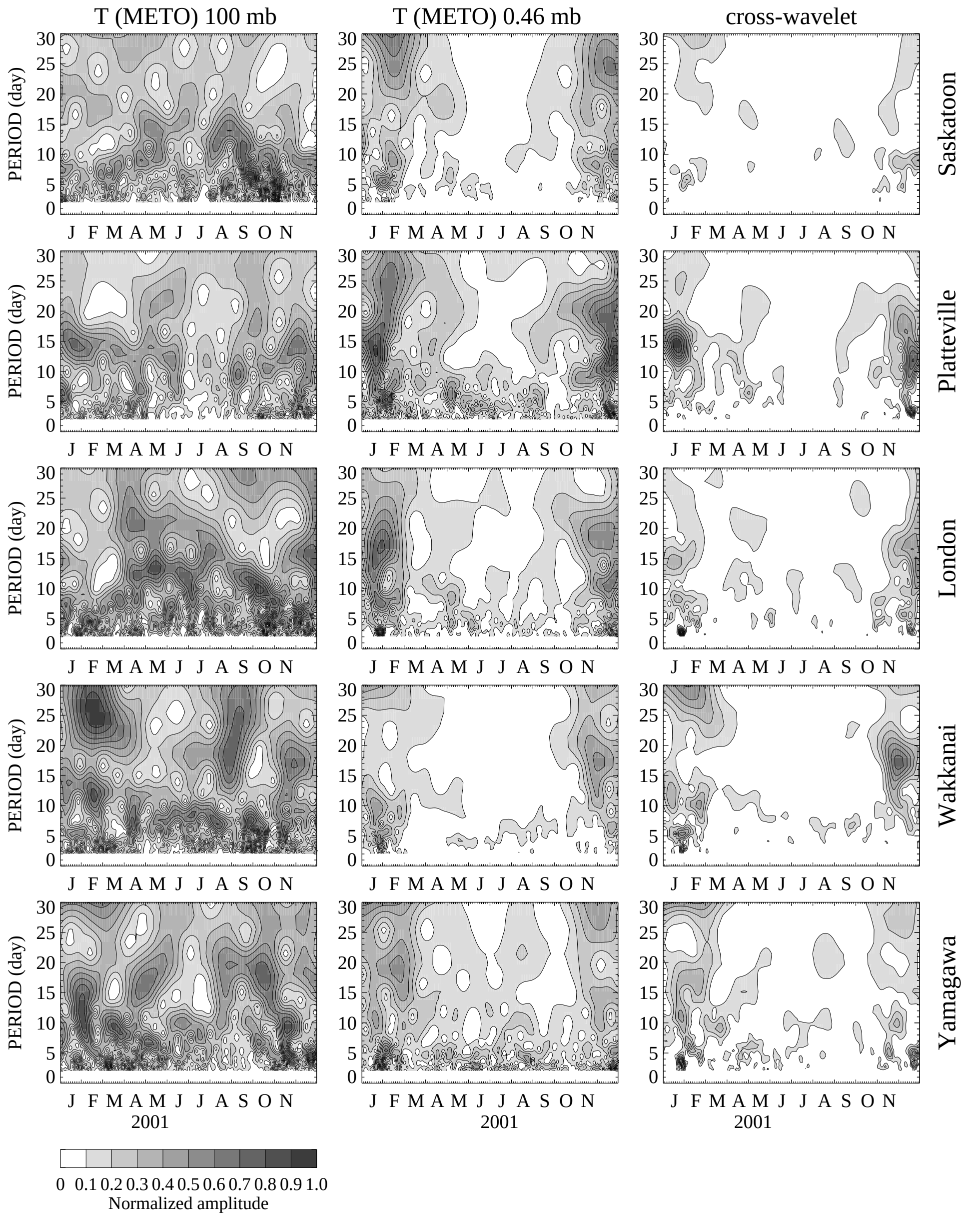

Fig. 5. The same as Fig. 4, but for MetO temperature at 100 mbar and 0.46 mbar pressure levels.

There are also relatively few features present on the plots for the lower level that also occur on the plots for 0.46 mbar. Actually, the height 20–25 km (22–46 mbar) divides the lower atmosphere into two regions (consistent with Fig. 2) where the spectral content is different. At Yamagawa this boundary is a little higher than at other four locations: London, Platteville, Saskatoon and Wakkanai. Zonal winds in this height range have lowest speeds (and the reversal from mainly eastward (below 20 km) to westward (above 25 km) in summer occurs there). Although such conclusions have been reached by others (e.g. Shepherd, 1992), the results are additionally pertinent here as later we will consider the wave numbers of these waves, and the differences in the directions of horizontal propagation at the two heights.

The lower spectral intensity at the higher altitude (0.46 mbar), especially in the long-period range in summer time, could be explained by the dependence of the associated planetary wave propagation on zonal circulation. Only waves with phase speeds that are westward relative to the mean flow, or waves whose phase velocities do not equal the flow at some height (Charney and Drazin, 1961) can propagate upward. Note that there is greater similarity between spectral features ($\geq$10 days) in the 0.46 mbar wavelets than at 100 mbar. Some common features, such as a signature of the 5-day period at the end of January (early February), appear at more than one station. Also, in the cross-products for mid-latitude stations, especially London and Platteville, there are similar energy distributions in wintertime. The cross-wavelet

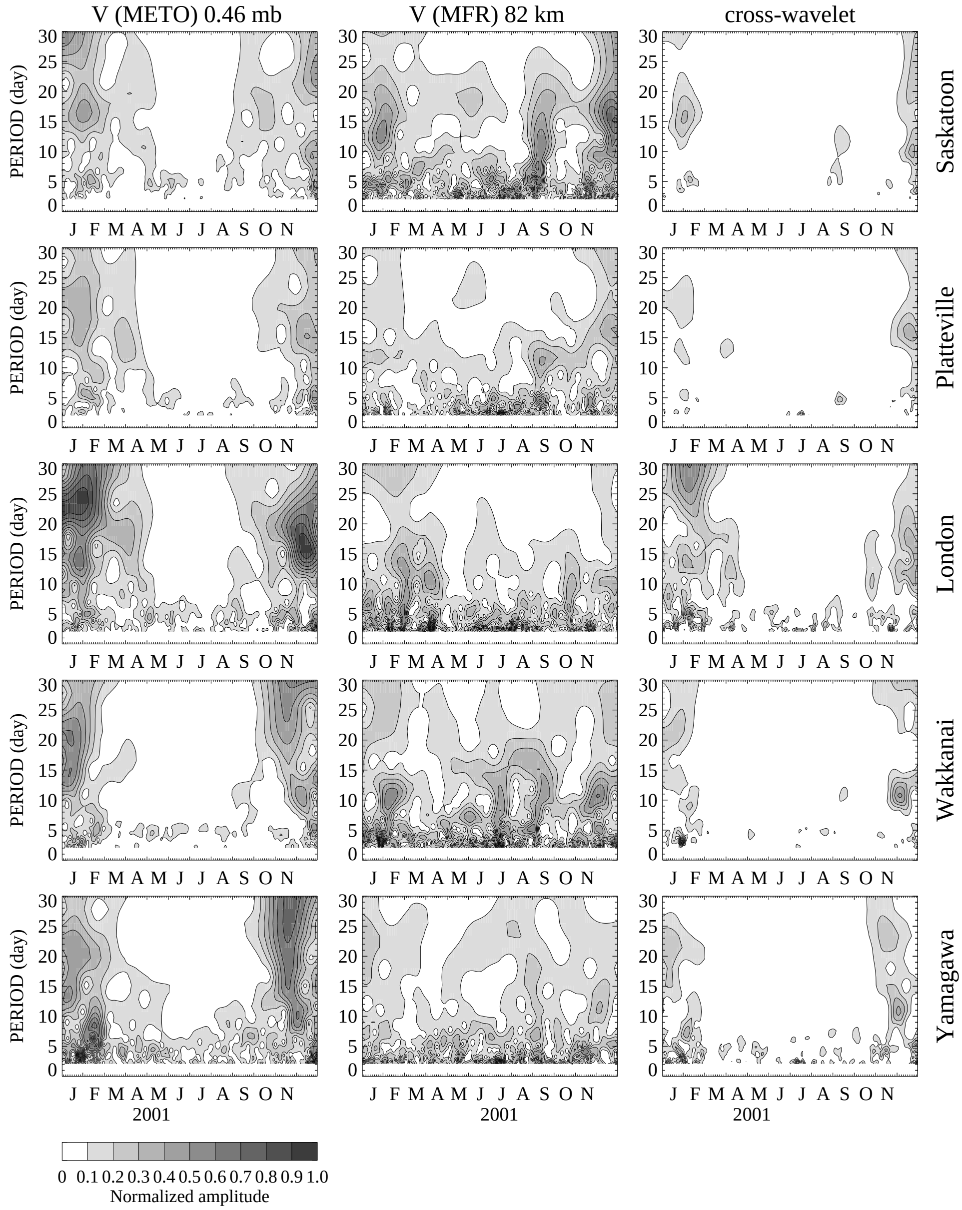

Fig. 6. (**a**) The self-normalized wavelet amplitudes versus time (2001 year) and period (2–30 days) calculated for the meridional component (V) of the MetO winds at 0.46 mbar (the left column) and MF radar winds at 82 km (the center column), and their cross-products (the right column) are presented for all five CUJO locations. From the top to the bottom these are for Saskatoon, Platteville, London, Wakkanai, and Yamagawa.

of the total ozone and temperature at 0.46 mbar is very similar to the cross-product of the temperatures from the two different heights shown here. (That is expected based upon comparisons shown in Fig. 4.)

The comparison of the wavelet spectra for the temperature (MetO) and wind (MetO) at the same pressure level show that they have some similarities as well as differences. Not all peaks present in the three parameters individually are present simultaneously in all three. Some of the peaks, such as those with long periods of 20–25 days in January/February at Saskatoon, can be found in 0.46 mbar temperature (the second column of Fig. 5) and zonal wind plots (the first column of Fig. 6b), while they are absent from the plots of the meridional wind (the first column of Fig. 6a); others, such as 5–6 day peak in December at Wakkanai is clearly seen in temperature and meridional wind, but not in zonal wind. Some peaks (20–25 days in January/February at London) are present in both components of the wind, but are not evident in the temperature. Despite this, the spectral distributions for T, U and V are quite similar in general structure at each site, i.e. months of enhanced wave activity and the related approximate periods of the spectral peaks are similar.

Finally we consider the winds from MetO at the 0.46 mbar pressure level (∼50 km) and from the MF radar at 82 km.

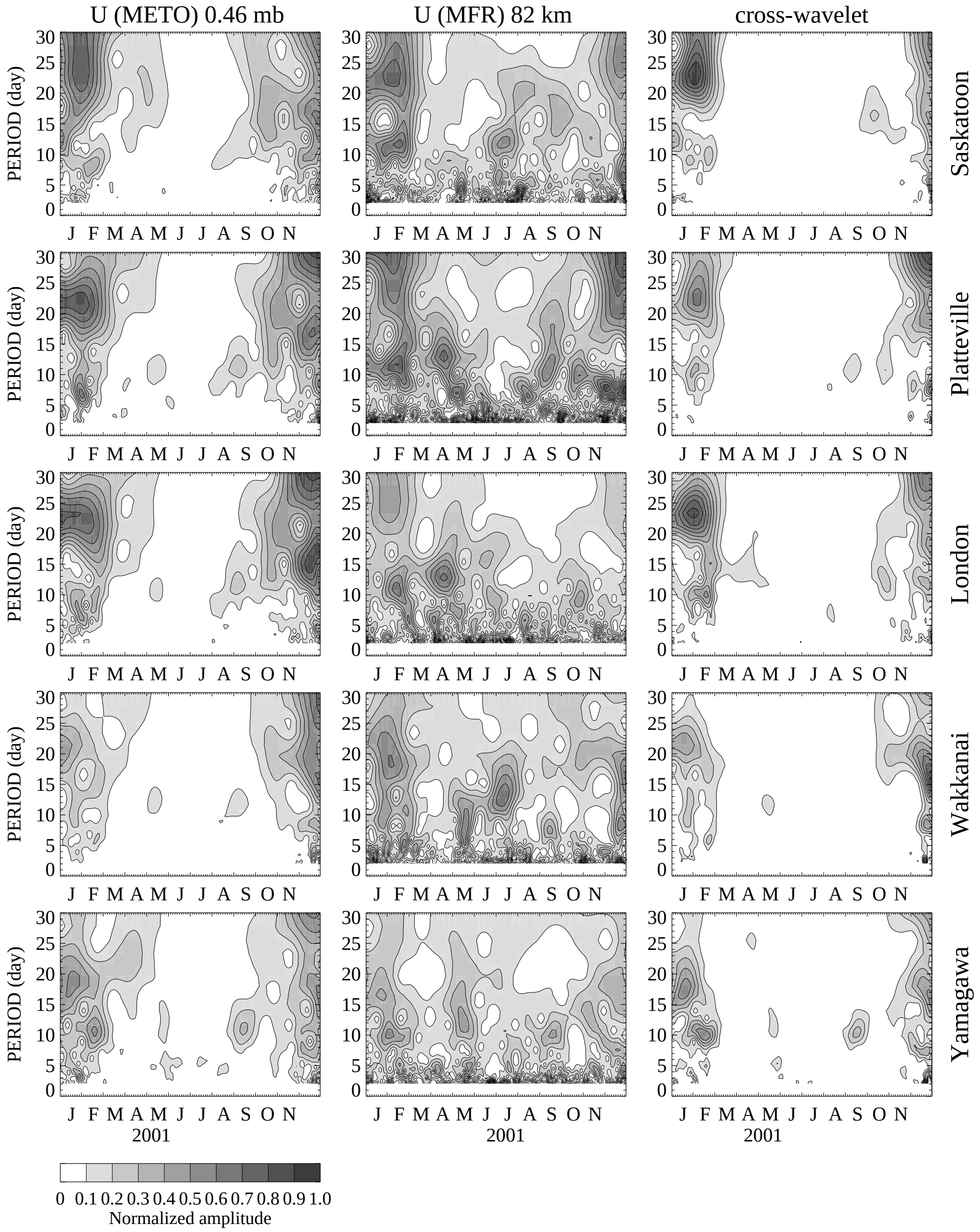

Fig. 6. (**b**) The same as Fig. 6a, but for the zonal (U) winds.

Figure 6 has been introduced already, but its main purpose is to compare winds at stratospheric and mesospheric heights. The meridional components are used in Fig. 6a and the zonal in Fig. 6b. It can be seen that the character of wave activity is changed again. More high frequency features appear in the MFR wind wavelets in contrast to those of the MetO winds at the lower (0.46 mbar pressure) level, and there is more mesospheric wave activity in summer months. This former may be due to more inherent smoothing in the MetO model. One common feature for both MetO and MFR zonal winds is a strong peak at 20–25 days in January/February that is present at all stations except Yamagawa. Actually the magnitude of this peak increases with height (i.e. before normalization) and it is not present or is very weak at MetO levels below ∼2.15 mbar (40 km). The cross-wavelets highlight these features. In the meridional winds there are some common peaks in the higher frequency range. Among others there are 5-day peaks in wavelets and cross-wavelets in January/February at Saskatoon and (more weakly) at Platteville. This was previously noted in the MetO temperatures (the second column of Fig. 5) and meridional winds (the first column of Fig. 6a). There is also a strong 2–4 day peak at Yamagawa and Wakkanai at the end of January and the beginning of February. It is also seen in the zonal wind component, but it is less prominent. The greater similarity in spectral features between the five locations of CUJO, at these upper heights (stratosphere-mesosphere), suggests larger scale waves and more global coherence. Larger zonal amplitudes are also

Fig. 7. (**a**) The same as Fig. 6a, but for the year 2002.

consistent with characteristics of normal modes (Luo et al., 2002b). Besides the common features there are differences in wavelets for different CUJO locations. These differences can be explained by latitudinal and longitudinal variations in the response of the atmosphere to the global normal PW modes (Manson et al., 2004).

The existence of 10–15 day peaks during summer months (June, July, 2001; Fig. 6b) in the zonal MFR winds at Saskatoon and Wakkanai is interesting, but not unusual (Luo et al., 2002a). It has been assumed that such summer activity could be due to the mesospheric dissipation of upward propagating gravity waves that are modulated at a period of near 16 days at stratospheric heights (Smith, 1996). However, no peaks with similar periods are present in the winds at this time at stratospheric heights (neither at 0.46 mbar, nor at 100 mbar). An alternative source could be in the Southern Hemisphere, and this possibility is assessed later in the next section. The absence of the burst at other locations at 82 km can be attributed to the intermittent nature of the 16-day wave and its dependency on the background winds (Luo et al., 2002b).

As was mentioned above, one year differs from another in the details of the dynamic activity. For example, MetO (0.46 mbar) and MFR (82 km) wind wavelets for year 2002 (Figs. 7a,b) have no strong spectral feature in zonal winds at long periods as was the case for the winter of 2000/01. Instead there is often spectral energy at the mid-latitude locations (82 km) at periods near 15 days in January and ∼10 days at the end of March. Consistent with this, there

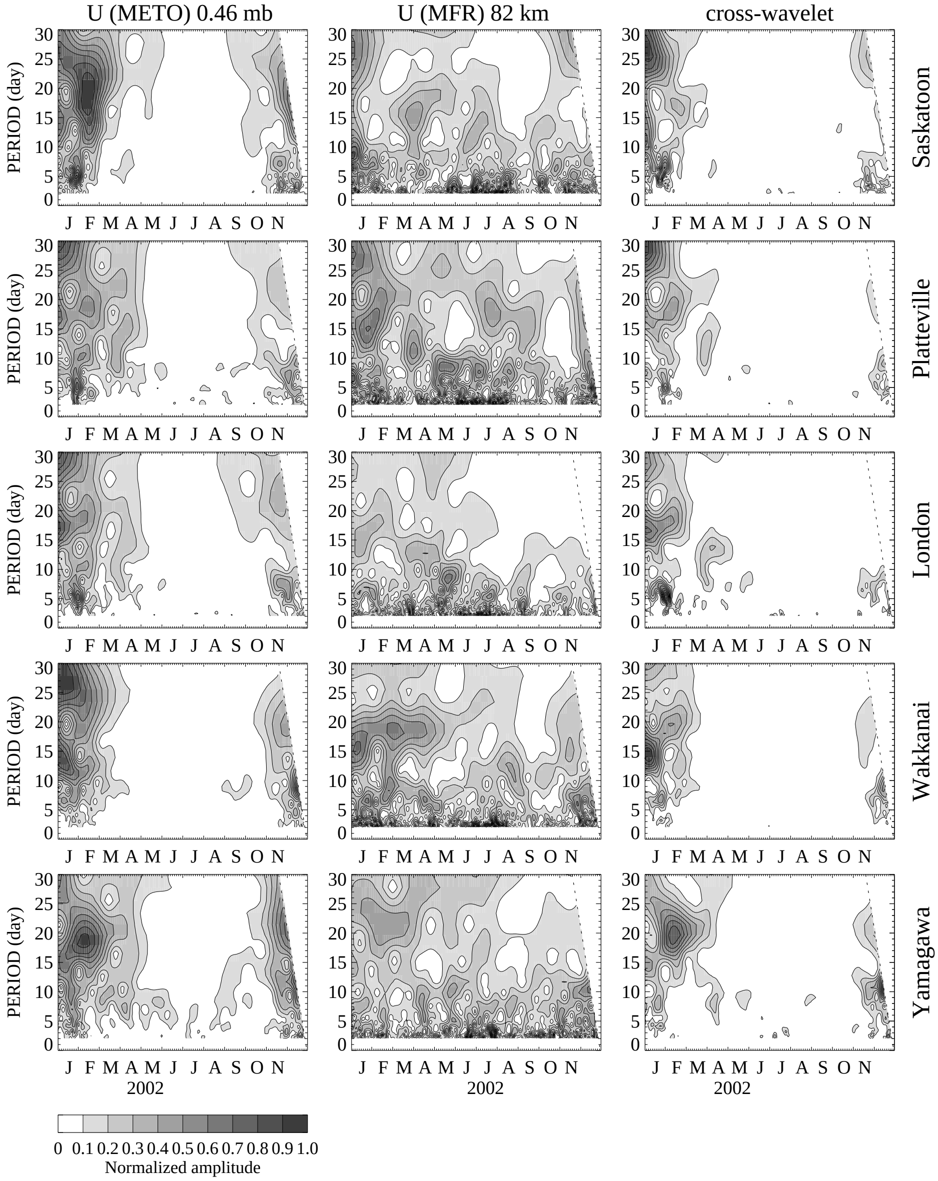

Fig. 7. (**b**) The same as Fig. 6b, but for the year 2002.

are peaks around 15 and 10 days in the zonal component of the MetO winds at the 0.46 mbar pressure level at some locations. Otherwise however, there is somewhat less consistency (period and time) between peaks at stratospheric and mesospheric levels, or between different locations, than during 2001. In the plots for the meridional winds, only the 5-day peak in January appears at all CUJO locations.

5 Wave number study

The assumed model is $V_{ij}=V\,cos\,(\omega t_j+mL_i-\phi_o)$ where V_{ij} is the wind measured at site i and time j, V is the planetary wave amplitude, L_i is the longitude (in radians eastward of 0°) of site i, m is the zonal wave number, ω is the wave frequency, and ϕ_o is the phase at zero longitude and zero time. A positive m indicates a westward propagating wave m=0 represents disturbances spread over the whole latitudinal circle (i.e. changes in zonal mean wind). There is no phase dependence on latitude, which means that the model assumes east-west planetary wave propagation. Firstly a Fourier transform of the time sequence, e.g. 90 days of MetO temperatures or winds, is done for each latitude/longitude bin, resulting in a complex amplitude at each frequency, latitude, and longitude. Then for each frequency and latitude a Fourier transform over longitude of these complex amplitudes is done, i.e. spatial Fourier transform, where the frequency now represents wave number (number of waves around the earth's circumference), and the sign of the frequency represents propagation direction, eastward or westward. These spectra are coherently integrated

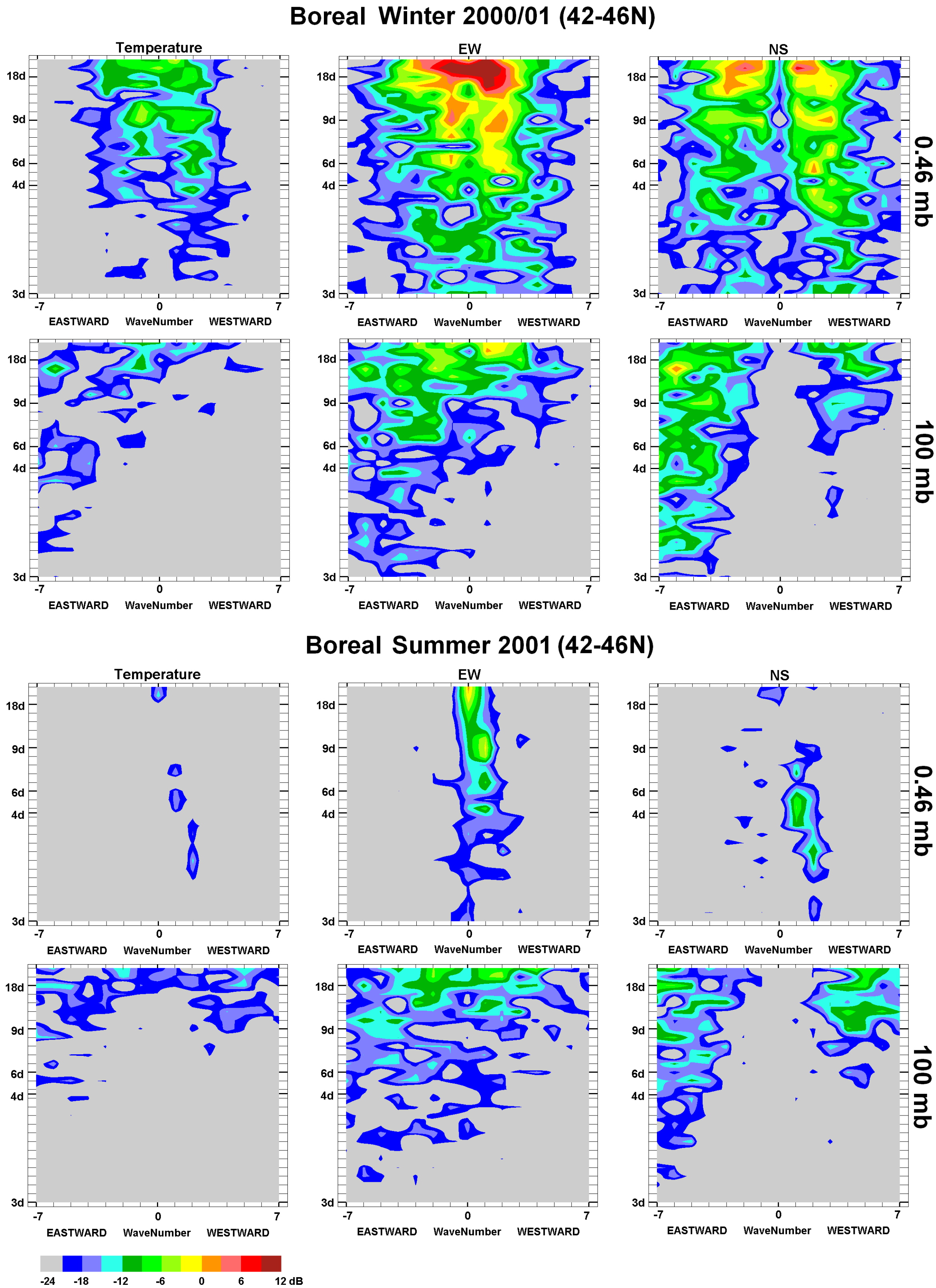

Fig. 8. Wave numbers versus frequency calculated for MetO temperatures (left), zonal, EW, (middle) and meridional, NS, (right) wind components at the 0.46 and 100 mbar pressure levels for 42–46 N latitude band during the 2000/01 winter (December 2000–February 2001) (two upper rows) and the 2001 summer (two bottom rows). Some periods are shown for convenience, the divisions are cycles per 90 days and range from 3 (top) to 30 (bottom).

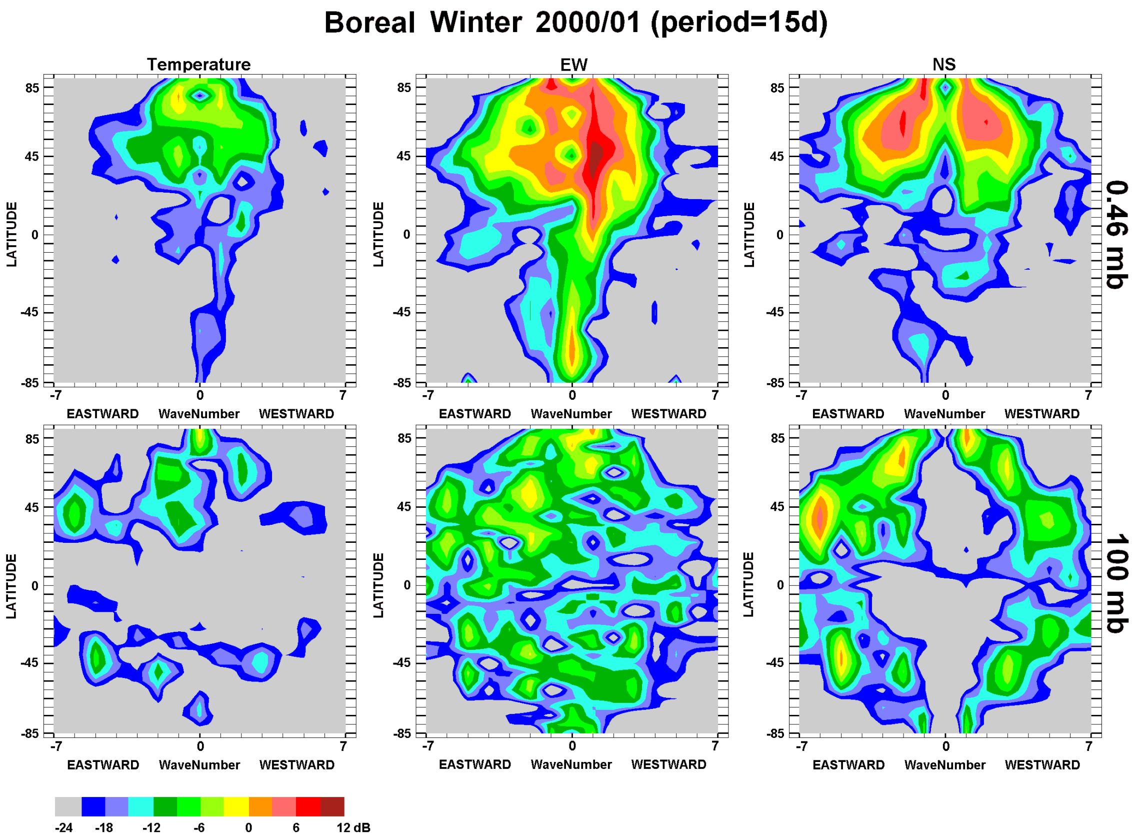

Fig. 9. Plots of wave number versus latitude for the oscillation with the period of 15 days in temperature (left), zonal, EW, (middle) and meridional, NS, (right) wind components at 100 mbar (at the bottom) and 0.46 mbar (at the top) pressure levels during 2000/01 boreal winter (December 2000–February 2001).

over the selected latitude band, e.g. 4 deg. Contour plots of their amplitudes over period (days) and wave number for a given sub-set of MetO temperature and winds have been prepared.

Figure 8 is for the 100 mbar and 0.46 mbar pressure levels during winter (December 2000–February 2001) and summer (June–August, 2001). In each part, the plots for MetO temperatures (left column) and zonal (middle column) and meridional (right column) components of the winds are presented for 42–46° N latitudinal band. The same dB levels are used for each plot of Fig. 8 for easy inter-comparison. The value in dB is equal to 20*$\log_{10}$ (wave amplitude in m/s and ° K).

Looking first at the 2000/01 winter (the two upper rows of Fig. 8), the three parameters have different patterns. At 100 mbar low wave numbers ($-2<m<2$) dominate in temperatures and zonal wind component, while in the meridional component there is a "valley" around m=0 (between eastward and westward directions) for all frequencies. The width of this "valley" depends on the height, so that the valley is wider at the lower 100 mbar pressure level than at 0.46 mbar. These patterns do not depend on the latitude; but on the other hand the amplitudes or intensities of the temperature and zonal wind contours at higher latitudes are larger than for low latitudes (not shown). Among all parameters the contours of the zonal component of the winds have highest amplitudes, especially in the low frequency range. The plots for the winter of 2001/02 (not shown) have quite similar characteristics.

Comparisons of the two pressure levels reveal two main differences. In the first place, at 100 mbar the MetO parameters have rich spectral content with dominant eastward motions; while at 0.46 mbar the spectral intensities for the westward motions become comparable to, or larger than, eastward motions. Secondly, the amplitudes are larger (more red colour, >0 dB) at 0.46 mbar than at 100 mbar for all components.

The wave activity varies with the season, which is clearly seen, for example, from the plots of the monthly average Eliassen-Palm flux divergences presented in the atlas of atmospheric general circulation (Randel, 1992). As expected, in Fig. 8 in summer (the two lower rows of the figure) there is much less wave activity at both levels (and for all locations 27–56° N). At the 100 mbar level the spectral energy is spread more evenly between eastward and westward wave numbers than it was in winter at this level, while at 0.46 mbar pressure level most of the contours are aligned along m=0 and +1. Compared to the winter, relatively more energy can

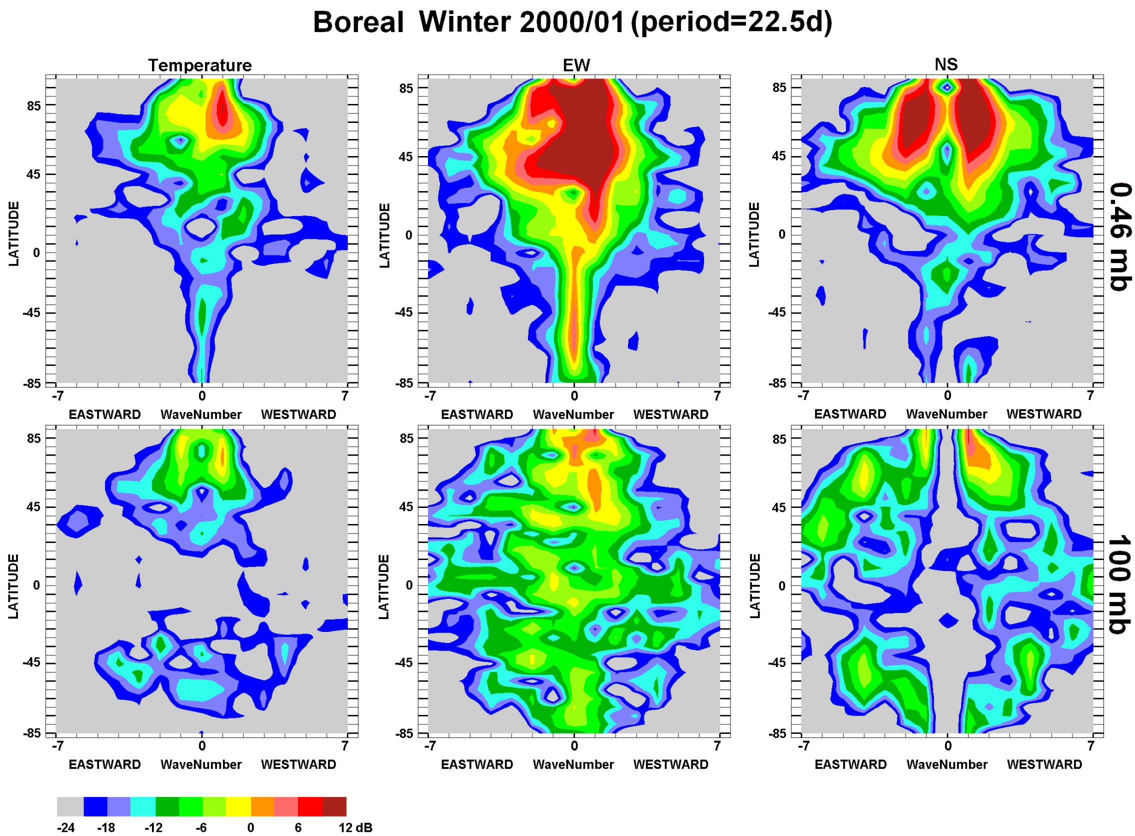

Fig. 10. The same as Fig. 8, but for the oscillation with the period near 22 days.

be found at high frequencies at 0.46 mbar level. As noted before (Sect. 4, Fig. 6b), there is no evidence of the mesospheric (82 km) 10–15 day oscillation in these wave number plots.

Now we focus upon a couple of the features, which it is believed could be associated with truly global events. The first feature is a 15 day eastward-propagating oscillation with the zonal wave number m=−6 in boreal winter 2000/01 (Fig. 8). Although the peak is strongest in the meridional winds at low latitudes (not shown), it is present in all parameters and all latitudinal bands at the 100 mbar pressure level. It seems that this oscillation does not propagate upward; at least the peak is not present at the 0.46 mbar pressure level. On the plots of wave number versus latitude for the oscillation with period near 15 days (Fig. 9) this feature is clearly seen as a bright red (in NS winds) or green (in EW winds and temperatures) area, which extends from the low to middle latitudes, at the 100 mbar pressure level (the bottom row). It is not present at the higher altitude (the upper row). Also, the 15-day peak can be easily identified at all CUJO locations except Saskatoon in Fig. 4 (comparison of the wavelets of the TOMS ozone and MetO temperatures at 100 mbar). In the TOMS wave number plots for January−February, 2001 (Manson et al., 2005, Fig. 7) the 15-day oscillation (4 cycles per 60 days) with m=−6 is also clearly seen for 39–44° N and 49–54° N latitudinal bands.

The second feature during the winter of 2000/01 involves the long period portion of the wavelets and wave number plots. This case is dominated by a peak near 22.5 days with m=+1 (westward). The long period oscillation (with T>20 days, Fig. 6b) has already been mentioned in Sect. 4 in connection with the 0.46 mbar zonal wind component. According to the wave number plots (Fig. 8) the peak maximizes at the higher (0.46 mbar) pressure level and is even stronger at higher latitudes (not shown). There is a signature of this oscillation at MF radar heights in the zonal winds as well (Fig. 6b) for most CUJO locations, and the cross-wavelets show the feature consistently. A frequency filter (20–40 days) was applied to the MFR and MetO (0.46 mbar) winds for this winter. The resulting time sequences (not shown) are complex, and consistent phase shifts between locations are difficult to establish except in January/February. However between Platteville/London and Wakkanai a wave number of 1.4–1.7 is estimated at the 82 km level. The filtered sequences at London, Platteville and Saskatoon (the three closest locations of CUJO network) are remarkably similar (as are raw data) at both levels, and close to zero phase shifts exist. On the plots of wave number versus latitude for the oscillation with period near 22.5 days (Fig. 10), the amplitudes are relatively strong along m=1 in the Northern Hemisphere as seen in all parameters and at both 100 mbar (bottom) and 0.46 mbar (top) pressure levels, strengthening and extending

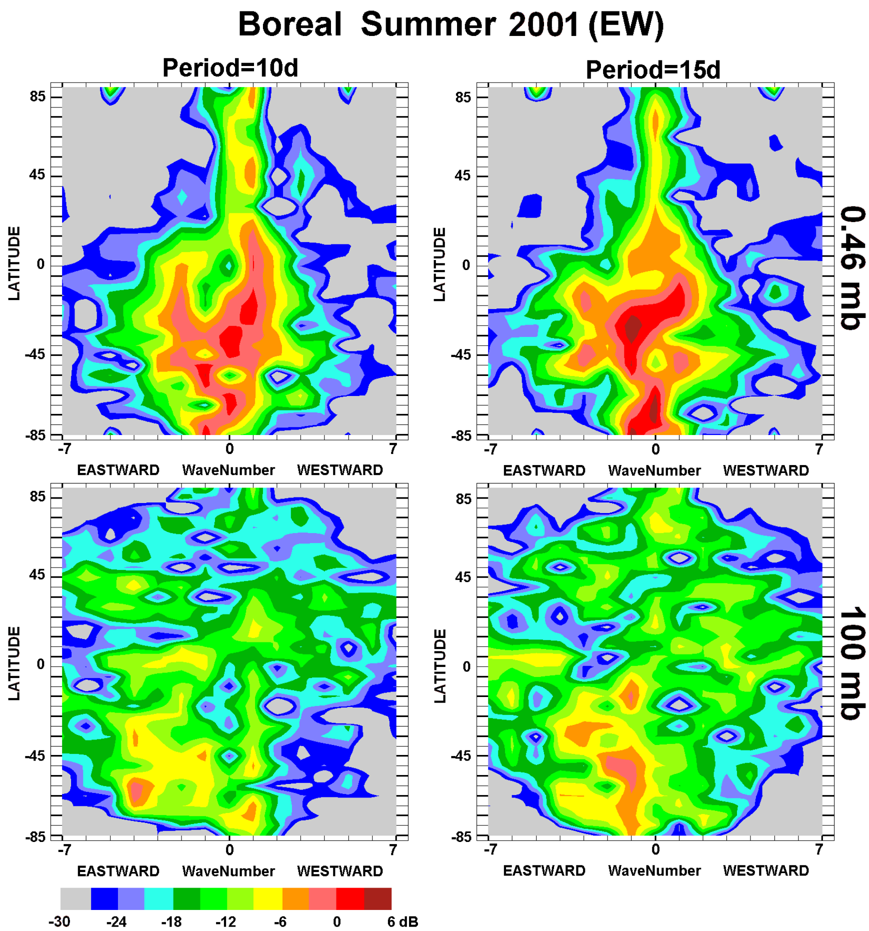

Fig. 11. Plots of wave number versus latitude for the oscillation with the period near 10 (left) and 15 (right) days in zonal (EW) wind components at 100 mbar (at the bottom) and 0.46 mbar (at the top) pressure levels during 2001 boreal summer (June–August 2001).

along low and middle latitudes at the higher altitude.

In the winter of 2001/02 (not shown) there is again no evidence for the ubiquitous 16-day wave with m=1. Although a "near 15-day" oscillation was observed in the MFR winds at mesospheric heights (discussion in Sect. 4), it shows little coherency between locations at stratospheric heights. Indeed MetO wavelets for other locations (Europe, Asia, and Pacific) along the 40° N latitudinal circle (not shown) did not consistently show this oscillation. The absence of the signature of the wave in the wave number plots can be explained by the fact that these calculations employ all grid points along the latitudinal circle rather than a few particular locations. Such intermittency and localization of 16-day oscillations is consistent with the planetary wave studies of Luo et al. (2002a), and the HRDI analysis of Burrage (see Luo et al., 2002b).

As one of the possible sources of the upper mesosphere 10–15 day disturbance, which is evident in the summer of 2001, ducting from the Southern Hemisphere has been named in Sect. 4 (Fig. 6b). In Fig. 11 plots of wave number versus latitude are shown for oscillations with periods near 10 and 15 days. The "patchy" picture at 100 mbar changes to a more elongated structure (extended along the wave numbers between −2 and +2) at 0.46 mbar pressure level. There is substantial spectral energy at m=+1 in the austral winter which could therefore be the stratospheric source of the 10–15 day oscillation observed in the Northern Hemisphere at this (northern summer) time. Differences between northern and southern hemispheric winters are also clear from Figs. 9 and 11. In general, the amplitudes are smaller in the Southern Hemisphere (note that the scales are different for the figures). Also, during the winter in the Northern Hemisphere eastward as well as westward motions are present at 100 mbar pressure level, while eastward motions largely dominate during the Southern Hemisphere winter. At the 0.46 mbar pressure level the amplitudes are greater and the westward direction is favoured during the boreal winter.

6 Summary

The coupling due to PW in the middle atmosphere (20–90 km) has been studied using TOMS, MetO and MFR data. To track similar spectral features from the lower stratosphere to the mesosphere wavelets have been calculated for all parameters at all available heights/pressure levels at five mid-latitude or extra-tropical locations in the North American-Pacific sector (CUJO network). Also, the wave number analysis has been applied to MetO parameters to separate eastward and westward propagating disturbances at stratospheric heights.

Comparisons and correlations between several parameters were completed:

1. High values of correlation and similar spectral features have indicated that of the MetO parameters, temperatures at low stratospheric heights (typically 100 mbar, 15–25 km) represent the total ozone best. This is consistent with the study by Schoeberl and Krueger (1983), which suggested that the variation of (total) ozone is a useful indicator of PW disturbances of medium zonal wave number near the tropopause.

2. The MetO (0.32 mbar, 55 km) and MFR winds (circa 60 km) are in good general agreement, especially for zonal component at particular mid-latitude locations. There are differences in values that could be attributed to the poorer reliability of the daily data parameter at the highest MetO and lowest MFR levels. The bias (small by a factor of ∼1.5) of the MFR winds was noted. This is the first comparison of its type between MetO and radar data.

The indications and characteristics of coupling from the lower to the upper middle atmosphere are as follows:

1. The annual variations of spectral content at PW periods change significantly between MetO 100 mbar (15–20 km) and 0.46 mbar (50 km) levels, consistent with much reduced PW activity at the upper level during the summer months. This can be attributed to the westward zonal winds of the middle atmosphere (e.g. Charney and Drazin, 1961; Luo et al., 2002). This is not a new result, in general form, but it is useful to demonstrate with the MetO data.

2. Based upon annual wavelet analyses for particular locations at low to middle latitudes, the spectral features of the MetO temperatures (T), zonal (U), and meridional (V) winds differ somewhat at the same level. [T and V are more similar for the periods less than 10 days. T and U have more in common at long periods (more than 12 days)]. Such behaviour is expected even for the classical “normal” planetary wave (PW) modes, due to different harmonic (Hough mode) structures (Forbes, 1995). This is important to keep in mind when comparing different parameters from different heights.

3. Spectral features common to MetO (0.46 mbar, ∼50 km) and MFR (82 km) heights, as indicated by wavelet and cross-wavelet analysis, are restricted to winter months and are typically of 15–25 day periods for the zonal and less than 10 day periods for the meridional components. Such strong events usually also provide evidence for the associated PW over a range of latitudes (10–15°) and, of course, longitudes; there may even be PW signals at 100 mbar.

4. Wave number analysis shows that the eastward motions dominate at low stratospheric heights, while westward motions became comparable or even stronger in the upper stratosphere/lower mesosphere. Earlier analysis (Manson et al., 2004) demonstrated westward motions at upper middle atmosphere heights (∼85 km). The eastward waves at the lower heights are dominated by small scale synoptic waves, which will be absorbed at greater heights (due to their small “critical speeds” (Charney and Drazin, 1961), or eastward motions relative to the background winds). The mean background wind also apparently plays an important role in determining the spectrum of waves that are able to propagate upward, especially due to the existence of critical levels (where wave phase speed is equal to background wind) in summer months. However, the increasing influence of westward propagating waves with height may be due to in situ generation (e.g. Lieberman et al., 2003) or a Southern Hemisphere source (Luo et al., 2002b).

5. It was also noted that at mesospheric heights there are more similarities in the characteristics of the wave activity between different locations (1000–7000 km in the CUJO network) compared to low stratospheric heights, where local weather phenomena dominate.

6. There are relatively few oscillations in the PW spectrum which can be followed from low stratosphere heights near 100 mbar (MetO) to the upper mesosphere near 82 km (MFR), and which are also hemispherically coherent (with well defined wave numbers). This is consistent with the intermittency in time and space of bursts of PW energy obtained at mesospheric heights. Although the three considered years (2000–2002) differ one from another in the details of the dynamic activity, the general results of comparisons are consistent from year to year.

Acknowledgements. Thanks are due to the UK Meteorological Office for the stratospheric assimilated data and to the British Atmosphere Data center for providing access to these data. We are also would like to thank the Ozone Processing Team, NASA/Goddard Space Flight Centre.

Topical Editor U.-P. Hoppe thanks a referee for his/her help in evaluating this paper.

References

Briggs B. H.: The analysis of spaced sensor records by correlation techniques, Handbook for Middle Atmosphere Program, 13, 166–186, 1984.

Burrage, M. D., Ortland, D. A., Skinner, W. R., and Hays P. B.: Direct measurements of global stratospheric winds from HRDI on UARS, Report, Space Physics Research Laboratory, Department of Atmospheric, Oceanic and Space Sciences, College of Engineering, University of Michigan, 1997.

Cervera, M. A. and Reid, I. M.: Comparison of simultaneous wind measurements using colocated VHF meteor radar and MF spaced antenna radar systems, Radio Sci., 30, 833–865, 1995.

Charney, J. G. and Drazin, P. G.: Propagation of planetary-scale disturbances from the lower into the upper atmosphere, J. Geophys. Res., 66, 83–109, 1961.

Forbes, J. M.: Tidal and Planetary waves, in The Upper mesosphere and Lower Thermosphere: A Review of Experiment and Theory, Geophysical Monograph 87, 67–87, 1995.

Hagan, M. E.: Comparative effects of migrating solar sources on tidal signatures in the middle and upper atmosphere; J. Geophys. Res. 101, 21 213–21 222, 1996.

Hocking, W. K. and Thayaparan, T.: Simultaneous and colocated observation of winds and tides by MF and meteor radars over London, Canada (43° N, 81° W), during 1994–1996, Radio Sci., 32, 833–865, 1997.

Hood, L. L., McCormack, J. P., and Labitzke, K.: An investigation of dynamical contributions to midlatitude ozone trends in winter, J. Geophys. Res., 102D11, 13 079–13 093, 1997.

Igarashi, K., Murayama, Y., Hocke, K., Yamazaki, R., Kunitake, M., Nagayama, M., and Nishimuta, I.: Coordinated observations of the dynamics and coupling processes of mesosphere and lower thermosphere winds with MF radars at the middle-high latitude, Earth Pl. Sp., 51, 657–664, 1999.

Kumar, P. and Foufoula-Georgiou, E.: Wavelet analysis for geophysical applications, Rev. of Geophys., 35, 385–412, 1997.

Lawrence, A. R. and Jarvis, M. J.: Simultaneous observations of planetary waves from 30 to 220 km, J. Atmos. Solar-Terr. Phys., 65, 765–777, 2003.

Lawrence, B. N. and Randel, W. J.: Variability in the mesosphere observed by the Nimbus 6 pressure modulator radiometer, J. Geophys. Res., 101, 23 475–23 489, 1996.

Lieberman, R. S., Riggin, D. M., Franke, S. J., Manson, A. H., Meek, C., Nakamura, T., Tsuda, T., Vincent, R. A., and Reid, I.: The 6.5-day wave in the mesosphere and lower thermosphere: Evidence for baroclinic/barotropic instability, J. Geophys. Res., 108D20, 4640, doi:1029/2002JD003349, 2003.

Lorenc, A. C., Bell, R. S., and MacPherson, B.: The Meteorological Office analysis correction data assimilation scheme, Quarter. J. Roy. Meteorol. Soc., 117, 59–89, 1991.

Lorenc, A. C., Ballard, S. P., Bell, R. S., Ingleby, N. B., Andrews, P. L. F., Barker, D. M., Bray, J. R., Clayton, A. M., Dalby, T. Li, D., Payne T. J., and Saunders, F. W.: The Met. Office global three-dimensional variational data assimilation scheme, Quarter. J. Roy. Meteorol. Soc., 126, 2991–3012, 2000.

Luo, Y., Manson, A. H., Meek, C. E., Thayaparan, T., MacDougall, J., and Hocking, W. K.: The 16-day wave in the mesosphere and lower thermosphere: simultaneous observations at Saskatoon (52° N, 107° W) and London (43° N, 81° W), Canada, J. Atmos. Solar-Terr. Phys., 64, 1287–1307, 2002a.

Luo, Y., Manson, A. H., Meek, C. E., Meyer, C. K., Burrage, M. D., Fritts, D. C., Hall, C. M., Hocking, W. K., MacDougall, J., Riggin, D. M., and Vincent, R. A.: The 16-day planetary waves: Multi-MF radar observations from the arctic to equator and comparisons with the HRDI measurements and the GSWM modelling results, Ann. Geophys., 20, 691–709, 2002b, **SRef-ID: 1432-0576/ag/2002-20-691**.

Manson, A. H., Gregory, J. B., and Meek, C. E.: Winds and wave motions (70–100 km) as measured by a partial reflection radiowave system, J. Atmos. Terr. Phys., 35, 2055–2067, 1973.

Manson, A. H., Yi, F., Hall, C., and Meek, C. E.: Comparison between instantaneous wind measurements made at Saskatoon (52° N, 107° W) using the colocated medium frequency radars and Fabry-Perot interferometer instruments: climatologies (1988–1922) and case studies, J. Geophys. Res., 101, 29 553–29 563, 1996.

Manson, A. H., Meek, C. E., Chshyolkova, T., Avery, S. K., Thorsen, D., MacDougall, J. W., Hocking, W., Murayama, Y., Igarashi, K., Namboothiri, S. P., and Kishore, P.: Longitudinal and Latitudinal Variations in Dynamic Characteristics of the MLT (70–95 km): A Study Involving the CUJO network, Ann. Geophys., 22, 347–365, 2004, **SRef-ID: 1432-0576/ag/2004-22-347**.

Manson, A. H., Meek, C. E., Chshyolkova, T., Avery, S. K., Thorsen, D., MacDougall, J. W., Hocking, W., Murayama, Y., and Igarashi, K.: Wave activity (planetary, tidal) throughout the middle atmosphere (25–100 km) over the CUJO network: satellite and medium frequency (MF) radar observations, Ann. Geophys., in press, 2005.

Meek, C. E.: An efficient method for analysing ionospheric drifts data, J. Atmos. Terr. Phys., 41, 251–258, 1980.

Meek C. E. and Manson, A. H.: Combination of Primrose Lake (54° N, 110° W) ROCOB winds (20–60 km) and Saskatoon (52° N, 107° W) MF radar winds (60–110 km): 1978–1983, J. Atmos. Solar-Terr. Phys., 47, 477–487, 1985.

Meek C. E., Manson, A. H., Burrage, M. D., Garbe, G., and Cogger L. L.: Comparisons between Canadian prairie MF radars, FRI (green and OH lines) and UARS HRDI systems, Ann. Geophys., 15, 1099–1110, 1997, **SRef-ID: 1432-0576/ag/1997-15-1099**.

Orsolini, Y. J., Limpasuvan, V., and Leovy, C.: The tropical stratopause in the UKMO stratospheric analyses: Evidence for a 2-day wave and inertial circulations, Q. J. R. Meteorol. Soc., 123, 1707–1724, 1997.

Pancheva, D., Mitchell, N., Middleton, H., and Muller, H.: Variability of the semidiurnal tide due to fluctuations in solar activity and total ozone, J. Atmos. Solar-Terr. Phys., 65, 1–19, 2003.

Randel, W.: Global Atmospheric Circulation Statistics, 1000–1 mb, NCAR/TN-366+STR, NCAR Technical note, National Center For Atmospheric Research, Boulder, Colorado, 1992.

Randel, W., Udelhofen, P., Fleming, E., Geller, M., Gelman, M., Hamilton, K., Karoly, D., Ortland, D., Pawson, S., Swinbank R., Wu, F., Baldwin M., Chanin, M.-L., Keckhut, P., Labitzke, K., Remsberg, E., Simmons, A., and Wu, D.: The SPARC intercomparisons of middle-atmosphere climatologies, J. of Climate, 17, 986–1003, 2004.

Remsberg, E., Lingenfelser, G., Harvey, V. L., Grose, W., Russell III, J., Mlynczak, M., Gordley, L., Marshall, B. T.: On the verification of the quality of SABER temperature, geopotential height, and wind fields by comparison with Met Office assimilated analyses, J. Geophys. Res., 108D20, 4628, doi:1029/2003JD003720, 2003.

Salby, M. L.: Fundamentals of Atmospheric Physics. International geophysical series v 61, Academic Press, 627, 1996.

Schoeberl, M. R. and Krueger, A. J.: Medium scale disturbances in total ozone during Southern Hemisphere summer, Bull. Amer. Met. Soc., 64, 1359–1365, 1983.

Shepherd, T. G.: Issues in stratosphere-troposphere coupling, J. Met. Soc. Japan, 80, 4B, 769–792, 2002.

Smith, A. K.: Longitudinal variations in mesospheric winds: evidence for gravity wave filtering by planetary waves, J. Atmos.

Sci, 53, 1156–1173, 1996.

Smith, A. K.: The origin of stationary planetary waves in the upper mesosphere, American Met. Soc., 60, 3033–3041, 2003.

Swinbank, R. and O'Neill, A.: A stratosphere-troposphere data assimilation system, Monthly Weather Rev., 122, 686–702, 1994a.

Swinbank, R. and O'Neill, A.: Quasi-biennial and semi-annual oscillations in equatorial wind fields constructed by data assimilation, Geoph. Res. Lett., 21, 2099–2102, 1994b.

Swinbank, R., Lahoz, W.A., O'Neill, A., Douglas, C. S., Heaps, A., and Pod, D.: Middle atmosphere variability in the UK Meteorological Office Unified Model, Quarter. J. Roy. Meteorol. Soc., 124 (549), 1485–1525, 1998.

Swinbank, R. and Ortland, D. A.: Compilation of wind data for the Upper Atmosphere Research Satellite (UARS) Reference Atmosphere Project, J. Geophys. Res., 108D19, 4615, doi:1029/2002JD003135, 2003.

Thayaparan, T., Hocking W. K., and MacDougall, J.: Middle atmospheric winds and tides over London, Canada (43° N, 81° W) during 1992–1993, Radio Sci., 30, 1293–1309, 1995.

Torrence, C. and Compo, G. P.: A practical guide to wavelet analysis, Bull. American Met. Soc., 79, 61–78, 1998.

Warner, C. D. and McIntyre, M. E.: Toward an ultra simple spectral gravity wave parameterization for General Circulation Models, Earth Pl. Sp., 51, 475–484, 1999.

Ziemke, J. R., Chandra, S., McPeters, R. D., and Newman, P. A.: Dynamical proxies of column ozone with applications to global trend models, J. Geophys. Res., 102D5, 6117–6129, 1997.